Computational study of competing reaction mechanisms of photo-catalytic reduction of CO_2 on anatase(101)

Chung Man Ip[†] and Alessandro Troisi[†,*]

[†]*Department of Chemistry and Centre for Scientific Computing, University of Warwick, UK*

Abstract

We perform a computational study of three different reaction mechanisms for the photo-catalytic reduction of CO_2 on TiO_2 anatase(101) surface known as (i) the carbene, (ii) the formaldehyde and (iii) the glyoxal pathway. We define a set of approximations that allows testing a number of mechanistic hypotheses and design experiments to validate them. We find that the energetically most favourable reaction mechanism among those proposed in literature is the formaldehyde path, and the rate-limiting step is likely to be the formation of CH_3 radical from dissociation of CH_3OH. We show that an intermediate that support this mechanism is OCH_2OH. We also find that formaldehyde would be an energetically favorable intermediate forming from CO and HCO, intermediates that are proposed in the early stage of the carbene and glyoxal pathways respectively. Some possible variants of mechanisms and method to ease the formation of CH_3 radical are also discussed.

1. Introduction

Photo-catalytic reduction of CO_2 with H_2O is a reaction that can produce storable fuels such as methane using clean and freely available solar power, as well as recyclable photo-active catalysts. This technology with sufficient efficiency should allow the formation of a reversible CO_2/CH_4 carbon cycle, which can potentially be a sustainable solution for the ever-increasing future energy demand.[1] Employing atmospheric CO_2 for this reaction would suggest that it may also assist regulating the concentration of atmospheric CO_2, which in turn should help mitigating climatic problems such as global warming.[2,3]

The operational principles of photo-catalytic reduction of CO_2 follow the general working principles for photo-catalysis.[4–6] The reaction is initiated by photo-excitation of the catalyst, which leads to the formation of photo-excited electrons and photo-holes in the bulk. The electrons and holes will migrate to the surface of the catalyst, and be available for redox reactions with surface species. In the initial stage of the conversion of CO_2 to CH_4, typical surface species for reduction are CO_2, surface protons and water.[7] The conversion is a reduction half-reaction and will require 8 protons and 8 electrons, or 8 hydrogen radicals, to complete:[8]

$$CO_2 + 8H^{\bullet} \rightarrow CH_4 + 2H_2O \qquad \text{(Eq.1)}$$

The 8 holes generated at the valence band edge of the semiconductor, e.g. TiO_2, should also react with surface species which would otherwise cause unwanted charge recombination with photo-electrons[5,9] and hinder reaction efficiency. In theory the holes can react with water to produce oxygen and protons:

$$4H_2O + 8h^+ \rightarrow 2O_2 + 8H^+ \quad \text{(Eq.2)}$$

In which the protons generated can be reduced to acquire hydrogen radicals. If we combine two half-reactions the total ideal reaction would be:

$$CO_2 + 2H_2O \rightarrow CH_4 + 2O_2 \quad \text{(Eq.3)}$$

The generation of oxygen (Eq. 2), however, is not commonly observed due to the difficult four-hole chemistry required. Therefore, additional hole scavengers, such as amines and alcohols, are typically employed to remove the surface holes and for studying the photo-reduction of CO_2 in isolation.[8] We will focus on the reduction half-reaction in this study (Eq. 1).

A number of outstanding problems, however, are to be resolved to put this technology into industrial practice. The formation rate of CH_4, one of the common measures for the efficiency, is extremely low, typically less than tens of μmol g^{-1} h^{-1}.[8,10] This is lower than, for instance, the hydrogen production rate of 19.8 mmol$g^{-1}h^{-1}$ in photo-catalytic water splitting using $NaTaO_3$:La(2%).[11] There is now a growing interest in developing new catalysts for improving the efficiency of this reaction, but very few general design rules[12–15] for new catalysts have been established. To systematically improve the performance of the catalytic system, it is essential to understand the reaction mechanisms on a commonly studied photo-catalyst, e.g. TiO_2, in order to identify the rate limiting step.

There is, however, no widely accepted reaction pathway for the chemical transformation of CO_2 to CH_4 on TiO_2, and effects of reaction conditions on the reaction mechanism are not well understood. Hitherto three main reaction pathways have been proposed for the photo-catalytic reduction of CO_2 on TiO_2 to gain CH_4, and they have been summarized in ref. 8. Here we report briefly the key intermediates in the mechanisms as described in ref. 8 with the evidence in support and the possible doubts that have been casted. The pathways, named in accordance with an intermediate along the pathway, are known as the carbene, the formaldehyde and the glyoxal pathway. These pathways mainly differentiate from one another after the presumable activation of CO_2 via one-electron reduction. In the carbene pathway,[16] the subsequent steps are the formation of CO, C residue, and a series of step-wise abstraction of 4 H radicals by the carbon to gain CH_4, in which carbene (CH_2) is expected in the last series of steps. In the formaldehyde pathway,[17] the main intermediates are formic acid (HCOOH),

formaldehyde (H_2CO) and methanol (CH_3OH), forming in this order along the pathway. The glyoxal pathway is the most complex pathway among the three proposed mechanisms, postulated based on a series of EPR experiments and DFT calculations.[18] After the activation of CO_2, it is expected that the HCO radical would form and dimerize to give glyoxal (HOCCOH). A series of electron and proton transfer thereafter lead to the formation of trans-ethane-1,2-semidione, glycol-aldehyde, vinoxyl radical and acetalaldehyde. The next step is a hole transfer to acetalaldehyde, to produce unstable acetyl radicals. The C-C bond in acetyl radical is then cleaved to give CO and CH_3, of which the latter can consume another H radical to produce CH_4.

While the proposed mechanisms appear to be reasonable based on chemical intuition and supported by some experimental evidence, there are details in each pathway that have not been elucidated or verified. For the carbene pathway, some important reaction intermediates (C, CH_3, CO, H) have been confirmed with EPR studies, and experimental data were able to fit with the kinetic model for this mechanism.[19] This mechanism, however, does not explain the absence of HCOOH, a competitive product to CO that has been reported earlier in the proposed formaldehyde pathway.[17] Although there are reports of C residual detected on surfaces,[20] in theory the formation of a carbon atom is expected to be a thermodynamically unfavorable process, and the reaction to form C from CO has not been verified.

For the formaldehyde pathway, the closed-shell products are commonly observed and supported by the electrochemical reduction potential data (Eq. 5 to Eq. 8, vs NHE, pH=7),[7] where reduction potentials of CO_2 to form a number of products (HCOOH, H_2CO, CH_3OH and CH_4) via multiple electron and proton transfer are generally less negative than the conduction band potentials of TiO_2 ($E = -0.50V$):

$$CO_2 + 2H^+ + 2e^- \rightarrow HCOOH \qquad E = -0.61V \qquad \text{(Eq.5)}$$

$$CO_2 + 4H^+ + 4e^- \rightarrow H_2CO + H_2O \qquad E = -0.48V \qquad \text{(Eq.6)}$$

$$CO_2 + 6H^+ + 6e^- \rightarrow CH_3OH + H_2O \qquad E = -0.38V \qquad \text{(Eq.7)}$$

$$CO_2 + 8H^+ + 8e^- \rightarrow CH_4 + 2H_2O \qquad E = -0.24V \qquad \text{(Eq.8)}$$

There is, however, no experimental evidence for multiple-electron transfer and it is more likely that the reaction proceeds via single-electron transfer, but the expected radical intermediates from these reductions are not observed.[8,21] Experimental data were also unable to fit the kinetic model of this pathway.[19]

The glyoxal pathway encompasses some possibilities that are not considered in the other two proposed pathways, including the formation of C_2 compounds as

intermediates, and having oxidation with the photo-generated hole as an elementary step. In addition, the proposed mechanism takes into account the formation of commonly observed products such as CO, H_2CO and CH_3OH, despite these intermediates are not included in the conversion pathway to CH_4. For H_2CO and CH_3OH, both species are expected to undergo oxidation with surface holes to generate HCO and CH_2OH radicals, taking mainly the role of sacrificial hole scavengers, and would not undergo one-electron reduction.[18,21] Therefore this proposed mechanism suggests the formaldehyde pathway would only occur with 2-electron 2-proton transfer reactions. The main weakness of this pathway is that glyoxal and glycolaldehyde have not been reported.[18] In the study with EPR that leads to the postulation of this pathway, the transformations of the radicals to molecules are not demonstrated, and the identification of the vinoxyl radical is rather tentative.[18] Table 1 summarizes the key points of the proposed mechanisms.

Table 1. Summary of the detected species in the proposed mechanisms, the supporting evidence and the uncertain details for the proposed mechanism.

Pathway	Detected species in proposed mechanisms	Supporting evidence	Uncertain details
Carbene	C, CO, H, CH_3OH, CH_4, CH_3[16]	EPR experiments; kinetic model fitting	Formation of C atom; No explanation on the absence/role of HCOOH
Formaldehyde	HCOOH, H_2CO, CH_3OH, CH_4[17]	Electrochemical reduction potentials	Lack of experimental support e.g. EPR; No explanation on the absence/role of CO
Glyoxal	CH_3, CH_4, H [7] $HCOCH_3$[22]	EPR experiments; DFT calculations	Glyoxal and glycolaldehyde are deduced from EPR,[18,23] but are not reported

Although there is no accepted mechanism, various views regarding some important aspects of the reaction, e.g. rate-limiting steps, have been advocated. It is generally believed that the activation of CO_2 is a difficult reaction to realize and it is likely to be the rate-limiting step, suggested also by the electro-chemical potential of $CO_2/CO_2^{\cdot-}$ ($E = -1.90V$). Adsorption of CO_2 on the surface seems to be able to make the reaction viable, but there are very few reports of such anion on TiO_2.[24] Some studies have

therefore suggested that the reduction of CO_2 may occur only under specific circumstances, e.g. when oxygen vacancies are introduced.[25,26] Another possible rate-limiting step for the reaction is the adsorption of reactants, where a pseudo-first order relationship has been observed between photo-reduction of CO_2 and initial CO_2 concentration.[27]

2. Theoretical studies in photo-catalysis

Computational studies offer a complementary tool to study reaction mechanisms, being able to test the plausibility of a given mechanism and to suggest further experiments to support the validity of a given hypothesis. A relatively large amount of theoretical work has been devoted to study photo-catalytic water splitting to generate hydrogen fuel, especially the oxygen evolution reaction (OER), which is the oxidation half-reaction that has a high over-potential.[28] For examples, Valdes et.al.[29] have employed the computational hydrogen electrode (CHE) method[30] and analyzed possible reaction mechanisms on rutile(110) with different surface terminations. Li et.al.[31] have determined the microscopic mechanisms for this reaction on 3 different anatase surfaces. They have concluded that the reaction is not sensitive to surfaces, that visible light provides sufficient energy to drive OER kinetically and demonstrated that the over-potential can be reduced by co-doping the catalyst with Mo and C or Nb and N. Shen et.al.[32] have performed *ab initio* molecular dynamics with DFT of photo-catalytic water-oxidation on a hydrogen-terminated GaN cluster, and they have proposed a possible reaction mechanism, as well as demonstrated that the photo-hole has enough energy to drive the OER. Some other theoretical work on photo-catalytic water splitting has been summarized in ref. [33].

Theoretical efforts are not limited to the mechanism of overall chemical transformation, but have also been applied to understand the mechanism of elementary electron and proton transfer reactions, such as sequential or concerted transfer, in e.g. OER. For instance, Chen et. al.[34] have studied the chemical dynamics of the first proton and electron transfer step of the OER with DFT-based first principle molecular dynamics, and showed that the mechanism of this step is a proton transfer (PT) step followed by an electron transfer (ET) step. They have also explained the influence of pH on the rate of OER, where PT is a rate-limiting step at low pH (pH < point of zero charge (pzc)) while at high pH the rate-limiting step is the ET. The barrier for ET at high pH is much lower than the barrier of PT at low pH and therefore the rate of OER is faster at high pH, where the surface is covered by hydroxide. Cheng et. al.[35] have devised an electronic and protonic energy level diagram and showed that the thermodynamical over-potential in OER is attributed mainly to the scattered alignment of the electronic levels, not to the component from deprotonation. The diagram is also

useful to understand a catalyst's activity/inactivity. Hammes-Schiffer et. al.[36] have developed a general formalism (four-state model) for proton-coupled electron transfer (PCET), which can be adapted to electrochemical PCET at metal-solution interface based on a number of assumptions,[37] and also can be applied to the design of molecular electro-catalysis.[38]

While there is an accumulating amount of theoretical studies on photo-catalytic water-splitting, there are comparatively much fewer studies on the photo-catalytic reduction of CO_2. Indrakanti et.al.[25] have studied the adsorption of CO_2 on small clusters using both post-Hartree-Fock and DFT methods, and they showed that transferring an excited electron from a stoichiometric TiO_2 surface to CO_2 is energetically unfavourable, but the charge transfer may be more favourable when oxygen vacancies are present. He et. al.[39] have studied 2-electron reduction of CO_2 on anatase(101), using a periodic slab model with the GGA+*U* scheme, and they have identified competitive pathways to form HCOOH and CO. In the same study a simple model was devised to screen a large number of dopants for lowering the reaction barriers. Recently Ji and Luo[40] have studied the formaldehyde pathway on the anatase(101) surface and proposed a new pathway, where CO replaces HCOOH in the formaldehyde pathway.

In this study, we consider three proposed mechanisms[8] of this reaction with a common set of approximations, and compute the reaction energy profiles for these mechanisms. Our main objective is to identify the most favorable pathway for this reaction. We first provide the computational method and the approximations in our model. We then show the reaction energy profiles of the mechanisms, and identify rate-limiting and other energetically unfavorable steps in each mechanism. In the discussion we compare the profiles of the three mechanisms, note possible mechanistic hypotheses, and suggest methods for verifying the identified pathway.

3. Computational method and model

All calculations are performed with GGA/PBE functional with ultra-soft pseudo-potentials with Quantum Espresso,[41] unless specified otherwise. The total energy of the intermediates are computed with anatase(101) surface, which is modeled as a two tri-layer slab with (2 × 2) surface unit cells. The two-layer slab is a rather thin slab but has been shown to be sufficient for modeling adsorption of molecule on the surface,[42] and we employ this slab also with the intention to save computational expense, in view of the rather large number of computations required in this study. For the most important results, where the thermodynamic landscapes of different pathways are being compared, we compute also the energies of the intermediates with a 5-layer slab for checking the main conclusions. The Monkhorst-Pack k-point grid used is 2 × 2 × 1, and the kinetic

energy cutoffs for wave-functions and charge density are 35Ry and 280Ry respectively.[42] For intermediates involving radical species, spin-polarized calculations are performed. The energies of the transition states are computed using the climbing-image nudged elastic band (CI-NEB) method.[43] We have first performed NEB based on an initial guess of the path, and subsequently improved the transition state energy of the NEB minimum energy path by using the climbing-image technique.

Our reaction (Eq.1) involves many reactants in sequence. To compare different reaction paths it is important to include the energy of the unreacted species in the intermediates' energy. To illustrate the procedure we consider the simple reaction:

$$CO_2 + 2H^{\bullet} \rightarrow CO + H_2O \qquad \text{(Eq. 9)}$$

We first compute the total energy of CO_2 adsorbed on the surface (denoted as (E_1)), which is the sum of the total energy of the surface adsorbate (CO_2), the surface slab employed and the associated adsorption energy. Similarly and separately, we compute also the total energy of a H atom adsorbed on the surface (E_H), which is the sum of the total energy of the H atom, the surface slab and the associated adsorption energy. The total energy of the reactant in Eq. 9, which is one adsorbed CO_2 and two adsorbed H atoms far away from CO_2 (E_{int1}), is simply:

$$E_{\text{int1}} = E_1 + 2E_H \qquad \text{(Eq.10)}$$

In the next step, we assume a H atom has diffused and is adsorbed close to CO_2, and we compute the energy of this configuration (E_2). The diffusion process is not studied explicitly. In addition, the total energy of the surface (denoted as *MS*) that has initially accommodated the diffused-away hydrogen (E_{MS}) is also computed. The total energy of this intermediate, which is one adsorbed CO_2 with one adsorbed H atom close to it and the other far away from it (E_{int2}), is:

$$E_{\text{int2}} = E_2 + E_H + E_{MS} \qquad \text{(Eq.11)}$$

Thereafter the total energy of COOH on the surface (E_3), as well as the transition state of the hydrogen transfer to produce COOH, are both computed and aligned with other intermediates by adding appropriate energies of E_H and E_{MS}. The same procedure is repeated until CO and H_2O are formed.

The elementary steps in the proposed pathways considered can have different mechanisms, such as sequential ET and PT, concerted PCET and hydrogen radical transfer, which may lead to the computation of an unmanageable number of possible intermediates for this study. We therefore model the photo-reduction process based on the hypothesis that the conversion from CO_2 to CH_4 proceeds via a series of H atom transfer reactions. In support of this hypothesis there is an expectation that H atom

transfer reactions very often exhibit low-energy barriers (less than 1.0 eV).[44,45] On the more practical side, this hypothesis would also allow a consistent computational setup to be applied for the three reaction mechanisms considered. We note that the Lowdin charge for an adsorbed H atom is typically ~0.6 in our calculations, and partial reduction of the TiO_2 slab is observed when there is no co-adsorbate. We have also observed that co-adsorbates are partially reduced when in the presence of a nearby adsorbed H atom (see SI for examples). We notice that the transfer of an adsorbed H atom has been considered as sequential ET and PT in some studies,[39,40] but in this study we will refer this process simply as H atom transfer.

Once reactants and products are connected via the computed intermediates under the hypothesis of sequential H atom transfer, it is possible to assess the potential impact of alternative sub-mechanisms connecting the same intermediates. If two reaction paths have relatively low barriers and very different energy of the intermediates, one can conclude that the lower energy intermediate path is more likely even if new lower energy paths connecting the intermediates could be found. If, on the contrary, the energy of the intermediates is similar and the reaction path is determined by the barrier heights, it becomes essential to study the detail of the rate determining steps. The approach presented here, depending on the results, will provide either the most likely mechanisms among those proposed or an indication of the elementary steps to be studied in greater detail.

The hypothesis of sequential H atom transfer requires some minor modification of the carbene pathway as described in ref. 8. We have considered alternative intermediates in this study to connect CO_2 to CO (connected via COOH) and CO to C atom (connected via HCO and HCOH) in the carbene pathway, to be compatible with our scheme. These alternative intermediates can be reasonably formed when an adsorbed H atom is close to the reactant on the surface (see SI for adsorption geometries), and/or have also been observed in other related reactions, which will be discussed in the results section. In the figures where our computed reaction pathways are defined we will use different representations to distinguish intermediates in proposed reaction pathways and intermediates suggested in this study.

Due to the rather large number of calculations required in this study, we have opted for the PBE functional for its relatively low computational cost. The adsorption energy of H atom on anatase(101), an important quantity to the relative energies in our energy profiles, may be dependent on the choice of functional. We have noticed that the PBE approach is able to produce the adsorption energies of H atom at the surface bridging O site of anatase(101) similar to that with the PBE+*U* approach (the difference is in between the range of 0.04 eV to 0.28 eV).[46,47] A limitation of the PBE approach is that the method is not able to describe localized excess electron, but pure, or non-adiabatic,

electron transfer reactions are not considered in this study. In additions, there are reports of both localization and delocalization of the excess electron in TiO_2 anatase,[48] and the localized and delocalization arrangements are found to be close in energy.[49] Hence localized excess electrons of the slab are deemed unimportant in this study. An accurate description of the localized states at the expense of higher computational cost, such as using DFT+*U*, would be needed when considering non-adiabatic electron transfer reactions.

4. Results

Carbene pathway

Fig.1 shows how the carbene pathway is defined in our study (the adsorption geometries of all the intermediates are reported in the SI). The pathway begins with the formation of CO **(8)** from CO_2 **(1)** via the formation of COOH **(4)**, a typical intermediate in the water-gas shift reaction on a solid surface.[50] CO then detaches from the surface and reacts with a H atom **(11)** to spawn HCO **(12)**, and a subsequent H atom transfer produces HCOH **(14)**. HCO is a common species detected in experiments[18] and HCOH is a species expected in carbene chemistry[51] and the photo-catalytic formation of carbohydrates.[52] HCOH is then rearranged to produce C atom and water **(16)**, and this C atom will sequentially abstract 4 H atoms on the surface to generate CH_4 **(26)**.

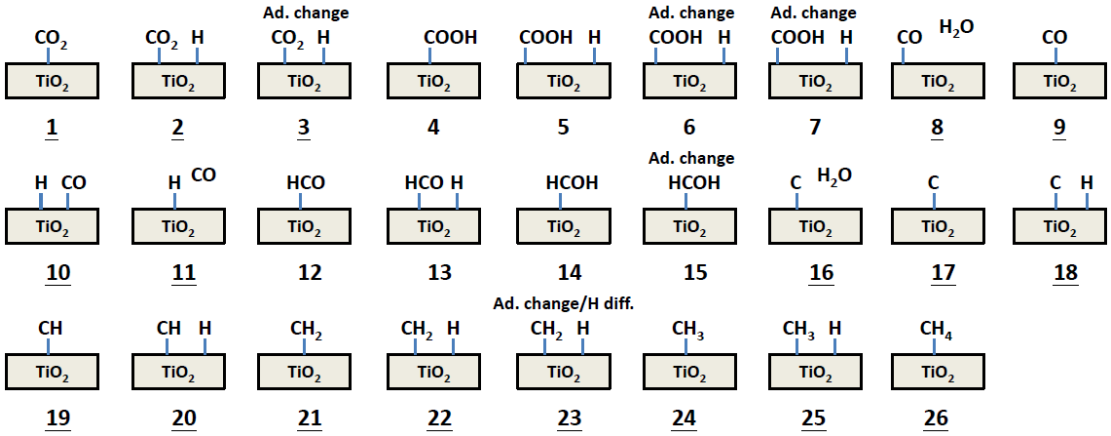

Fig. 1 Illustration of the intermediates involved in the carbene pathway in this study. 'Ad. change' means the intermediate has undergone adsorption mode and/or site change. 'H diff.' means diffusion of H atom between sites close to the adsorption of the intermediate. The underlined intermediates include species in the proposed reaction pathway,[8,16] while other intermediates are suggested in this study.

Fig.2 shows the energy profile of the carbene pathway. The solid black lines denote the energies of the intermediates, the blue solid curves denote the kinetic barriers, the blue dashed lines represent the processes where hydrogen diffuses and adsorbs close to the intermediate, or a water molecule diffuses away from the intermediate, for which

the barrier is not computed. The zero energy in Fig. 2 corresponds to the linear adsorption of CO_2 on anatase(101) **(1)**.

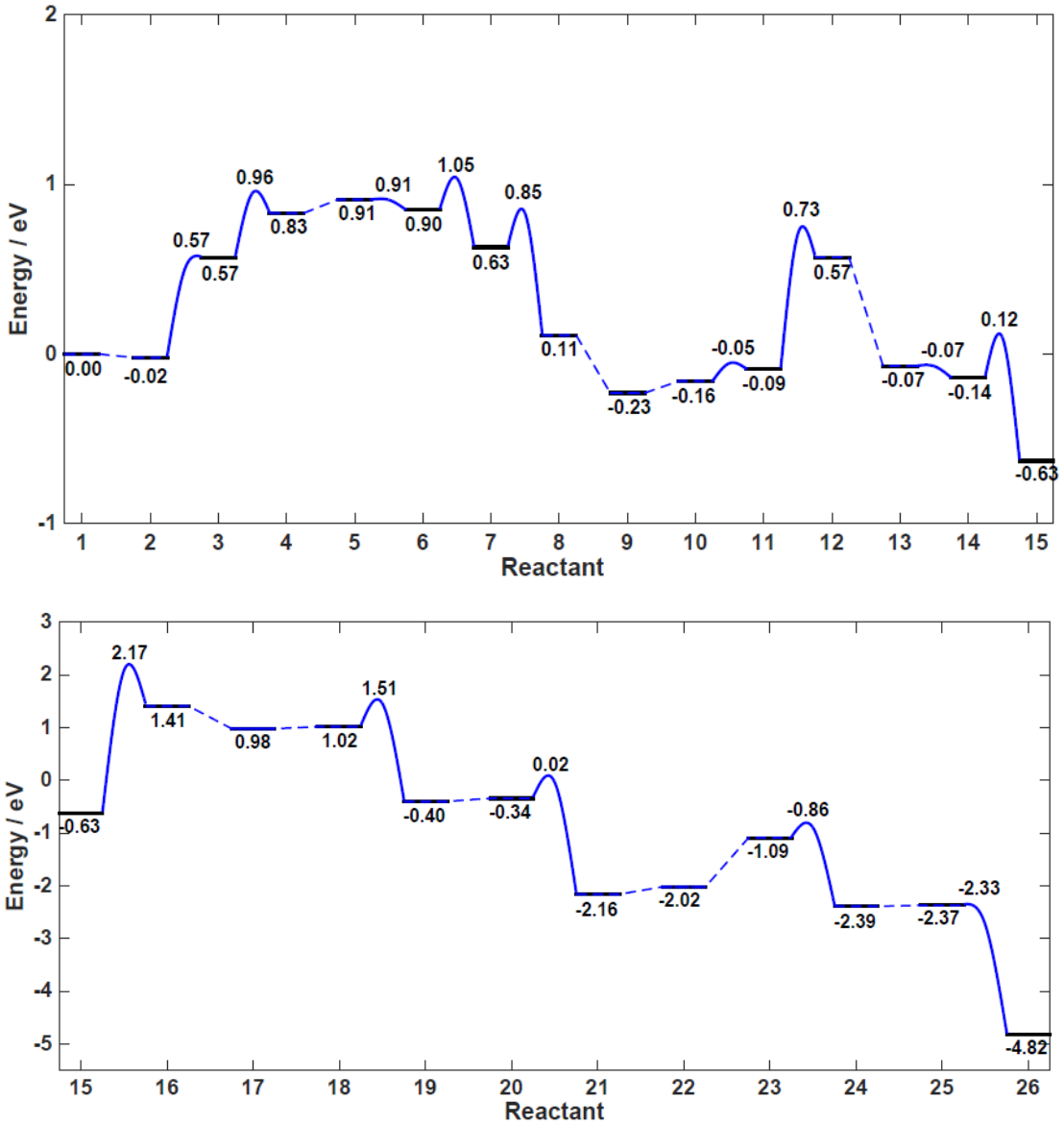

Fig. 2 Energy profile of the Carbene pathway. The energy profile in the top panel is magnified along the energy scale.

We first note that the rate-limiting step is the formation of a C atom from HCOH **(15 to 16)**, which is both thermodynamically (total energy difference (ΔE_{tot}) of 2.04 eV) and kinetically (kinetic barrier height (E_{act}) of 2.80 eV) unfavorable. Other possible paths to form C atoms, e.g. CO + H_2O + e^-,[53] are not examined. Once the C atom is formed, the subsequent H-atom abstraction goes steeply downhill. It should be noted that the ease of these H atom abstractions are related to the adsorption geometries of the carbon-based radicals. For instances, if the carbon atom of CH_2 is bonded to both a

surface unsaturated Ti atom and a bridging O atom, the abstraction of a H atom will have to be facilitated by breaking the C-O bond **(23)** (see SI for adsorption geometry); we are also unable to identify a reasonable transition state geometry for H atom abstraction by CH_3, when CH_3 is strongly adsorbing on a surface unsaturated Ti atom via the carbon atom.

In the course of building the energy profile for the carbene pathway the computation of kinetic barriers is the most time-consuming component, which essentially limits the number of reaction paths that can be explored. There has been endeavor to establish simpler and quicker methods to determine rate-limiting steps without computing explicitly the kinetic barriers. For instance, some heterogeneous catalytic reactions[44,54] have been found to obey the Bells-Evans-Polanyi (BEP) relation,[55,56] a linear relationship established between reaction barrier and reaction enthalpy change, and hence the barriers of reactions of the same families that obey BEP relation can be computed easily. Norskov et. al. have developed the CHE method[29,30,57] that allows estimation of the over-potential and the rate-limiting steps based on the assumed linear relationship between kinetic barrier and free energy difference, which appears sometimes to be an acceptable estimate.[33]

To investigate whether the energetics of the intermediates alone is sufficient for identifying the rate determining step and assessing the plausibility of different reaction mechanisms, we reported in Fig. 3 the activation energy E_{act} against the ΔE_{tot} for all H atom transfer (both forward and backward) reactions. This is the main type of reactions that we will consider when constructing the energy profiles for the formaldehyde and glyoxal pathways. The black lines indicate the minimum acceptable activation energies (since $E_{act} \geq \min(0, \Delta E_{tot})$). It can be seen that high activation energies (1.0 eV to 2.8 eV) are always associated with very positive ΔE_{tot}, and the difference, $E_{act} - \Delta E_{tot}$, is much smaller than the typical range of activation energies. BEP-type relationships for H atom transfer reactions have in fact been observed in the past.[44,45] This suggests that ΔE_{tot} often contains enough information to identify the slower steps in a reaction mechanism. More quantitatively, we could consider the following criteria to determine whether it is necessary to compute the kinetic barriers in the other two proposed pathways: (i) if the energy profile contains only the energies of the intermediates, and the resulting thermodynamic landscape is completely 'downhill' ($\Delta E_{tot} < 0$) or with 'uphill' steps having small ΔE_{tot}, e.g. $\Delta E_{tot} < 0.5$ eV, it would be necessary to compute the kinetic barriers in order to determine the rate-limiting step, as well as the potential maximum to assess the plausibility of the proposed reaction mechanism; (ii) If, however, the greatest ΔE_{tot} is > ~ 1eV, the energetics of the intermediates is likely to be sufficient to determine the rate-limiting step. We will then compute the barriers for this likely rate-limiting step identified in each pathway.

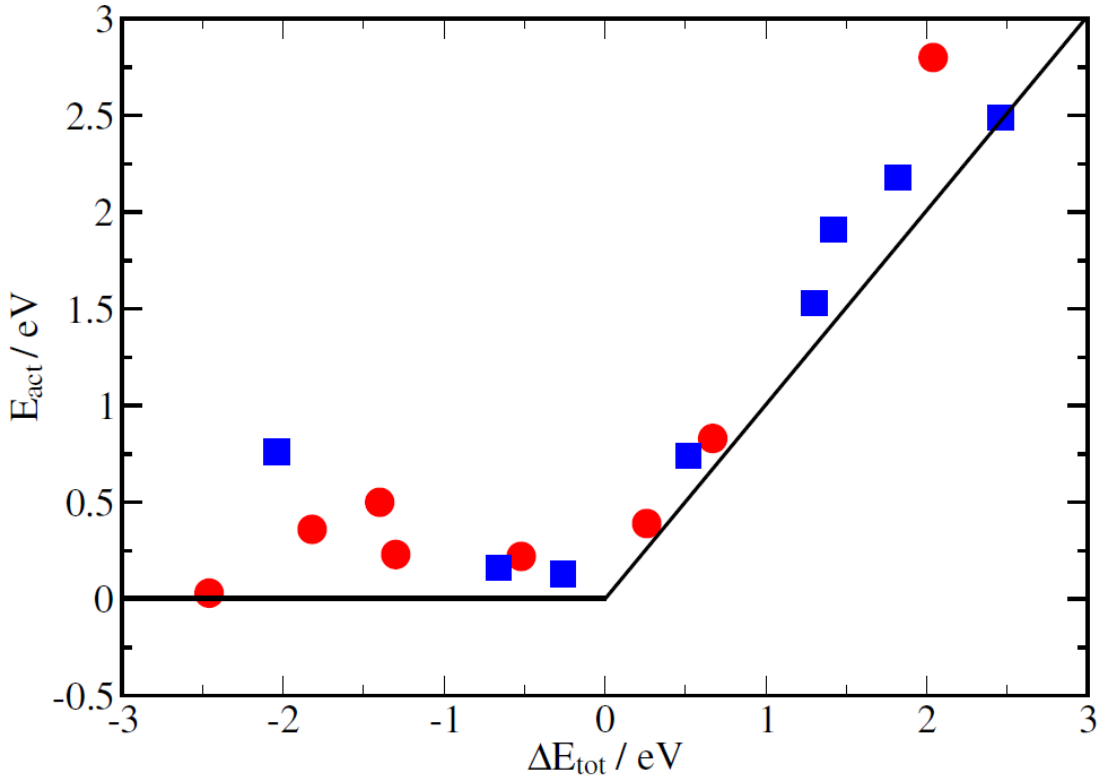

Fig. 3 Correlation between ΔE_{tot} and E_{act} computed based on energies of the intermediates and transition states of H atom transfer reactions presented in Fig. 2. The red circles are E_{act} of the forward reactions (8) and the blue squares are E_{act} of the backward reactions (8).

Formaldehyde pathway

Fig. 4 shows the intermediates in the formaldehyde path in this study and the energy profile of this pathway. The path starts with the formation of HCOOH **(5)** from linearly adsorbed CO_2 **(1)** via the formation of HCOO **(4)**. Subsequent step-wise abstractions of H atoms yield OCH_2OH **(8)**, H_2CO **(9)**, H_2COH **(12)**, CH_3OH **(14)**, CH_3 **(16)** and CH_4 **(20)**, in this order. Notice that, unlike other intermediates included in this pathway (**Table 1**), OCH_2OH **(8)** and H_2COH **(12)** have not been detected experimentally.[8] Note also that, for the formation of HCOO **(4)** and OCH_2OH **(8)**, we have placed an extra H atom on the surface (**(3)** and **(7)**) before H atom transfer. This is due to the observation that, while the energies between intermediates with and without a co-adsorbed H atom nearby are typically very similar, such as intermediates **(1)** and **(2)** in Fig. 4, HCOO **(4)** and OCH_2OH **(8)** are much lower in energy in the presence of an adsorbed H atom nearby than when adsorbed H atom is absent. The adsorption of two H atoms on the surface, such as intermediates **(3)** and **(7)**, has been used as a model for the initial state of two-electron 1-proton transfer reaction in DFT+*U* study elsewhere,[39,40] but we will

consider this as a H atom transfer, since only a partial reduction of reactant is observed, as discussed previously in Computational method and model.

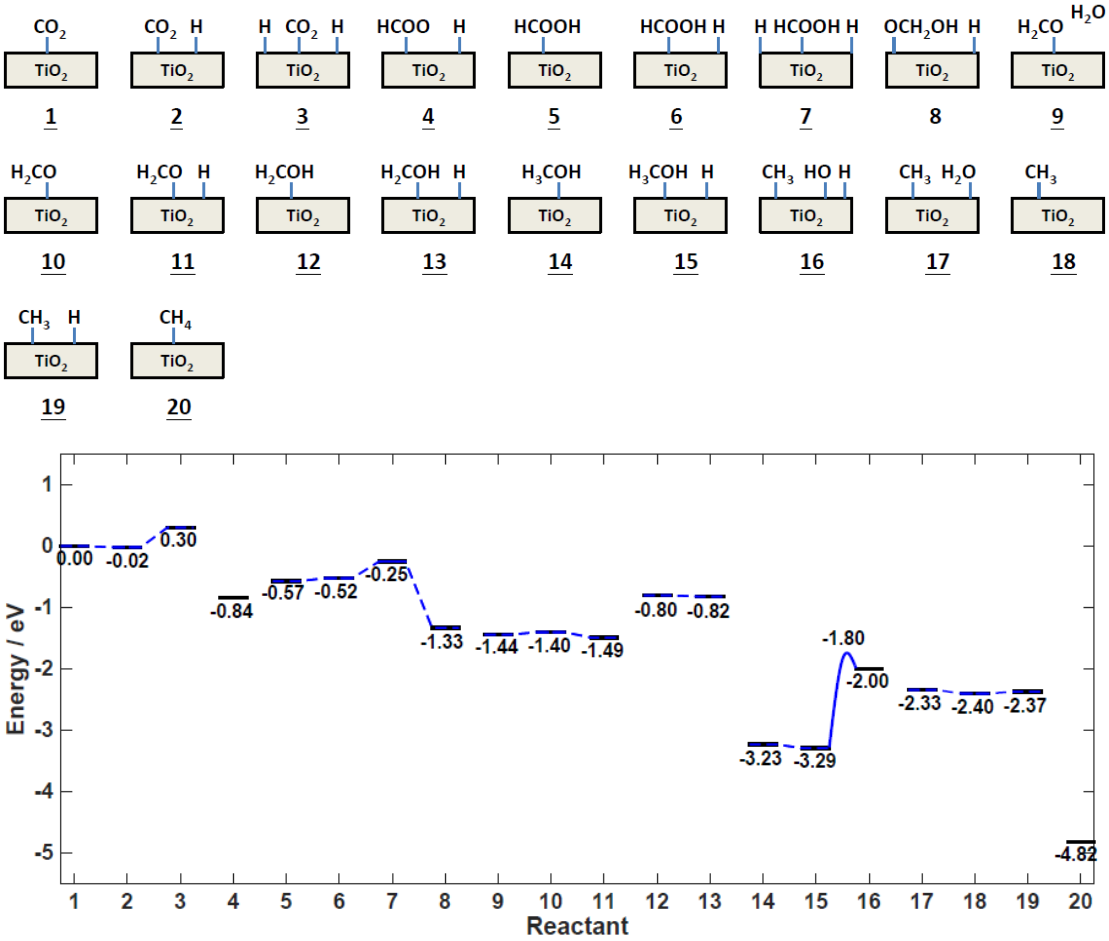

Fig. 4 (Top) Illustrations of the intermediates involved in the formaldehyde pathway in this study. The underlined intermediates include species in the proposed reaction pathway,[8,17] while other intermediates are suggested in this study. (Bottom) Energy profile of the formaldehyde pathway.

The rate-limiting step is likely to be the formation of CH_3 (**15 to 16**). The ΔE_{tot} of this step is 1.29 eV, and the E_{act} is 1.49 eV. The second most unfavorable step is the H atom transfer to H_2CO (**11 to 12;** ΔE_{tot} = 0.69 eV)**.** Considering the criteria given previously, it has been determined that the computation of kinetic barriers is not necessary for this pathway, except for the rate-limiting step. It should be noted that the energies of the most thermodynamically stable adsorption mode for HCOOH[58] and H_2CO[59] are not used in Fig. 4. In this case we have employed adsorption modes that can abstract a H atom without requiring changes in adsorption geometry or site that can yield OCH_2OH **(8)** and H_2COH **(12)**.

It has been suggested in ref. 21 that H_2CO **(9)** and CH_3OH **(14)** are acting mainly as

hole scavengers.[21] From Fig. 4 it can be seen that it is more thermodynamically favorable for H_2CO **(9)** to form the oxidation product OCH_2OH **(8)** rather than being reduced to gain H_2COH **(12)**, which is in agreement with ref. 21. Similar preference to form oxidation product H_2COH **(12)** by CH_3OH is however not observed from Fig. 4. Such observation is in line with some experimental results. For instance, in ref. 21 CH_3OH has much weaker hole-scavenging power among other tested species such as H_2CO; a temperature-programmed desorption (TPD) experiment[60] has suggested that methoxy, rather than molecularly adsorbed CH_3OH, is the effective hole-scavenging species in photo-oxidation of CH_3OH on TiO_2. Although in Fig. 4 the driving force for the forward reaction **(15 to 16)** is more favorable than the backward **(14 to 13)**, the former is still highly thermodynamically unfavorable, which suggests CH_3OH **(14)** is more likely a product or by-product rather than an intermediate, a feature that has also been considered in the proposed carbene pathway.[8] The relative stability of CH_3OH would also suggest that this species is likely to be involved in other side reactions, such as the indirect photo-oxidation, which is an oxidation mechanism of CH_3OH that is equally supported in comparison to the direct oxidation,[61] and/or the molecular CH_3OH react with co-adsorb oxygen to generate methoxy.[60] As such CH_3OH may take mainly the role of a hole scavenger.

Glyoxal pathway

We first note that in the glyoxal pathway CO is generated but not acting as a reaction intermediate. The fate of CO is however, not clear, where in theory it can also re-enter into the reaction cycle and act as an intermediate to produce CH_4. This postulation is supported by the general observation of CO being a typical minor or trace product, unless co-catalyst or propan-2-ol is employed.[8] Therefore, in accordance with our postulation, when CO is formed in the reaction of:

$$2CO_2 + 10H^{\bullet} \rightarrow CH_4 + 3H_2O + CO \qquad \text{(Eq.12)}$$

It reacts with H atoms and produces CH_4:

$$CO + 6H^{\bullet} \rightarrow CH_4 + H_2O \qquad \text{(Eq.13)}$$

and the total reaction is the doubling of Eq.1. For the purpose of correctly aligning the energies of the intermediates and constructing an energy profile that is comparable with those of the other two pathways, we consider a total reaction which is the sum of (half) (Eq.12) and (Eq.13). The resulting ΔE_{tot} between the initial reactant, CO_2, and the final product, CH_4, would therefore be the same as computed for the other two proposed pathways shown previously (-4.82 eV). The mechanism of converting CO to CH_4 is, however, not studied, since they are not provided in the proposed pathway. In this case

we would add a 'virtual step' of direct conversion of ½ CO to ½ CH_4 after the formation of the first ½ CH_4 in the profile.

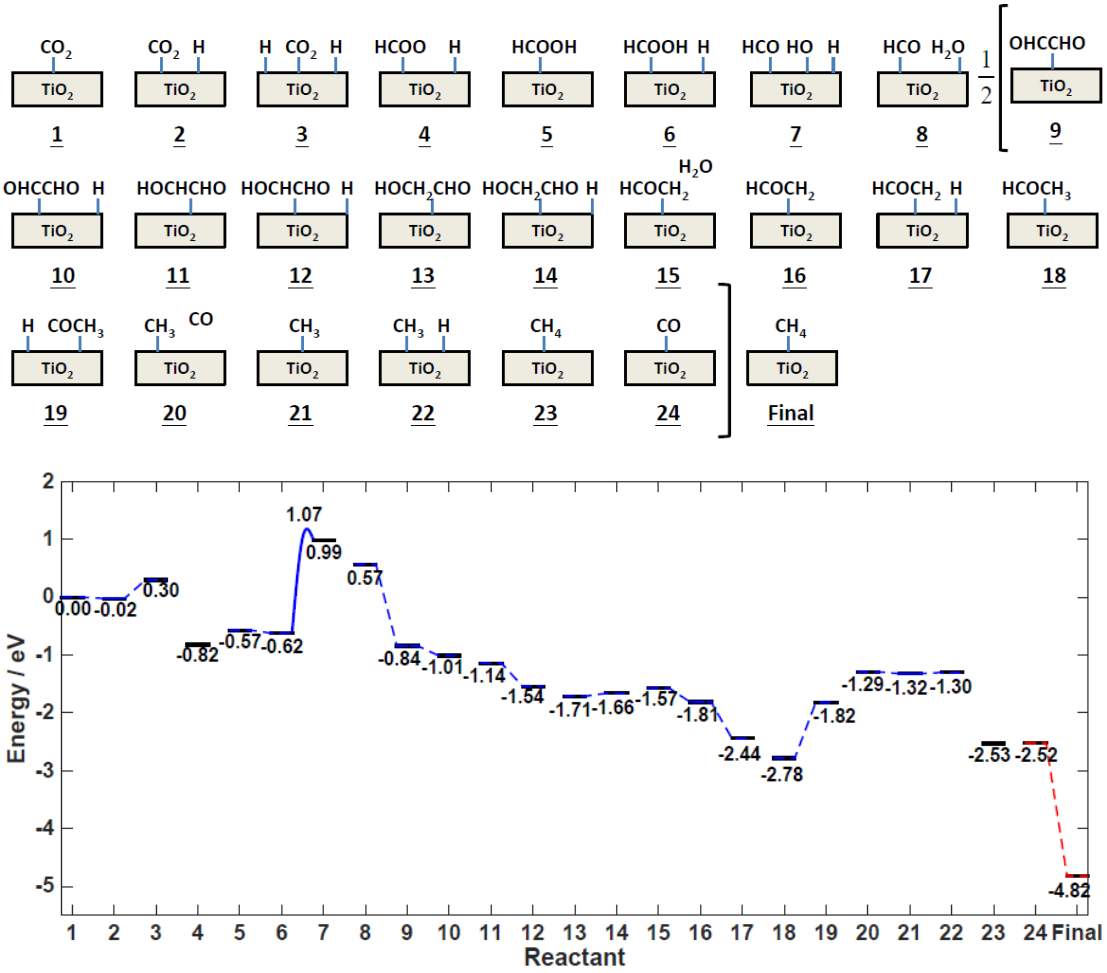

Fig. 5 (Top) Illustrations of the intermediates involved in the Glyoxal pathway in this study. The '½' brackets indicates the energies of which intermediates are halved. The underlined intermediates include species in the proposed reaction pathway,[8,18] while other intermediates are suggested in this study. (Bottom) Energy profile of the glyoxal pathway.

Fig. 5 shows how the glyoxal path is defined in this study and the energy profile of this pathway. The red dashed line connects the initial (½ CO + 3 H) and final state (½ CH_4 + ½ H2O) of the 'virtual step', in which the intermediates in between are not studied. The reaction begins with the formation of HCO **(7)** from linearly adsorbed CO_2 **(1)** via the formation of formic acid (HCOOH) **(5)**. Glyoxal (OHCCHO; **(9)**) is then produced from the dimerization of HCO **(7)**. The subsequent step-wise H atom abstraction produces trans-ethane-1,2,-semidione **(11)**, glycolaldehyde **(13)**, vinoxyl radical **(15)** and acetaldehyde **(18)**. The acetaldehyde **(18)** is then transformed to give acetyl radical and a H atom **(19)**. Thereafter the acetyl radical **(19)** is cleaved to form

CO and methyl radical **(20)**, which further abstracts a H atom to generate CH_4 **(23)**. The reaction is complete when CO released **(20)** re-enters the reaction cycle **(24)** and generates CH_4 **(Final)**.

From Fig. 5 it can be seen that the rate limiting step is likely to be the formation of the considerably unstable HCO (**6 to 7**). The ΔE_{tot} of this step is 1.61 eV, and the E_{act} is 1.69 eV. The second most unfavorable step is the formation of CH_3 from acetaldehyde (**18 to 19;** 0.96 eV). Similar to the formaldehyde pathway, by considering the criteria given previously, we have omitted the computation of kinetic barriers for this pathway, except for the rate-limiting step. We also note that acetaldehyde **(18)** would be the preferred product over ½ CH_4 **(23)** and ½ CO **(20)**, but if ½ CO **(20)** is allowed to be further reduced the product of this mechanism would be CH_4 **(Final)** only. From Fig. 5 acetaldehyde **(18)** is relatively stable on the surface, but it is a rather rare product.[8,22] This suggests acetaldehyde **(18)** is also likely to be involved in other side reactions, hindering the conversion to CH_4 **(Final)**. The mechanism in Fig. 5 would also be consistent with the difficulty of detecting glyoxal **(9)** and glycolaldehyde **(13)**,[18] as there is currently, to the best of our knowledge, no report of these species.

5. Discussion and Conclusion

Fig. 6 shows the simplified version of the three proposed pathways, where only important intermediates from H atom transfer reactions are included. Fig. 6 was constructed based on computation of intermediates with a two-layer slab; a comparison with this figure based on a five-layer slab sees our qualitative conclusions remaining unchanged, and this comparison is given in the SI.

From Fig. 6 it is evident that the formaldehyde pathway is the most thermodynamically favorable pathway, where the energies in general go 'downhill' from one closed-shell product to another **(0^{th} → 2^{nd} → 4^{th} → 6^{th} → 8^{th} H transfer, blue)**, whereas high-energy intermediates are involved in the other two pathways (HCO **(1.5^{th} H transfer, green)** in the glyoxal pathway and COOH/C **(1^{st}/4^{th} H transfer, red)** in the carbene pathway). An observation is that H_2CO **(4^{th} H transfer, blue)** is a favorable 'stepping stone' for all proposed pathways; it is seemingly more favorable for CO in the carbene pathway **(2^{nd} H transfer, red)** and the HCO in the glyoxal pathway **(1.5^{th} H transfer, green)** to form H_2CO rather than a C atom **(4^{th} H transfer, red)** and glyoxal **(3^{rd} H transfer, green)** respectively. The formation of H_2CO from CO has also been suggested in other DFT studies of CO_2 methanation on Cu surface[57] and anatase(101) surface.[40]

We have also tested the dependence of our identification of the most favourable pathway on our chosen functional. We have computed the reaction energies between CO_2 and the highest-energy intermediates in each pathway with PBE + U (U = 4.0 eV)[40]

and a five-layer slab, and compared them. The reaction energies in the carbene, glyoxal and formaldehyde pathways were 2.12 eV, 1.91 eV, and 1.21 eV respectively, and formaldehyde pathway should remain as the most favorable pathway.

We also noted that the uncertainty in our comparison of reaction mechanisms due to the introduction of some alternative intermediates for the carbene pathway **(1st and 3rd H transfer, red)** is deemed unimportant. The highest-intermediate in the carbene pathway is the C atom **(4th H transfer, red)**, which is much higher in energy than the intermediates in the formaldehyde pathways. This observation would not be influenced by considering alternative intermediates in the carbene pathway.

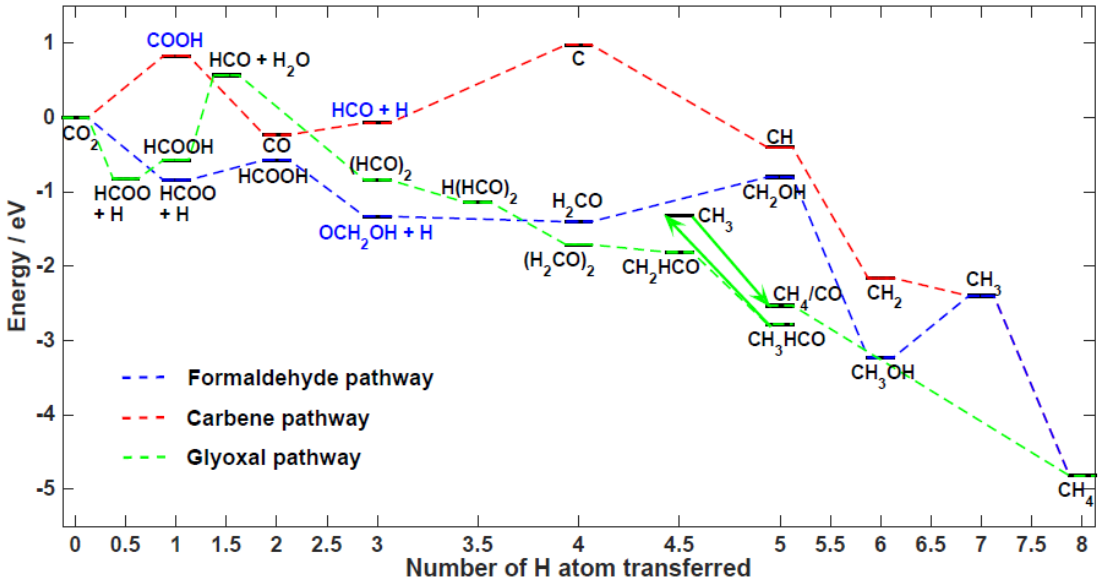

Fig. 6 Comparison of the intermediates' energy for the carbene (red), formaldehyde (blue) and glyoxal (green) pathways. The green arrow from the 5th to the 4.5th H atom transferred indicates CH_3HCO loses a H atom to form CH_3, and the green arrow from the 4.5th to the 5th H atom transferred indicates CH_3 regains a H atom to form CH_4. Note that the region of 3rd to 5th H atom transferred is magnified. Intermediates with'+ H' and '+ H_2O' means a H atom or a H_2O molecule co-adsorbs on the surface with the species. Intermediates in proposed reaction pathways are labeled in black, and intermediates suggested in this study are labeled in blue.

Our observations based on Fig. 6 should be verifiable with currently available experimental techniques. For instance, according to the results in Fig. 6, OCH_2OH **(3rd H transfer, blue)** should be easier to be detected than other radical species **(5th and 7th H transfer, blue)** in the formaldehyde pathway, and the identification of this species together with the following closed-shell products would be important supporting evidence for this pathway. OCH_2OH has been identified in the reaction between atomic

hydrogen and formic acid in Kr matrix with IR spectroscopy,[62] giving rise to an IR signal, e.g. an intense band at around 3600 cm^{-1} due to O-H stretching. The assignment of the IR spectra may be simplified by using other versions of IR spectroscopic technique, e.g. polarization modulation infrared reflection adsorption spectroscopy (PM-IRAS).[63] The conversion of CO and HCO to H_2CO would require kinetic modeling and/or isotope labeling techniques for verification.

From Fig. 6, we would also expect the main bottleneck for the formaldehyde pathway to be the unfavorable formation of CH_3 **(6^{th} → 7^{th} H transfer, blue)**. A new catalytic system should therefore improve the ease with which the C-O bond of CH_3OH cleaves. Alternatively, without changing the catalyst, the cleavage of this C-O bond may be facilitated by adding hydrogen iodide to react with CH_3OH in order to generate CH_3I. TPD experiment showed that the adsorption of a CH_3I layer on TiO_2(110) would produce CH_4.[64] CH_3I is also known to dissociate to produce CH_3 on other surfaces.[65,66]

We have noticed, on the basis of Fig. 6, two possible alternative sub-pathways that would avoid this unfavorable step. The first possibility is that H_2CO produces CH_2 instead of CH_3OH; but such reaction, to the best of our knowledge, is not known from literature. The second possibility is that the formaldehyde pathway proceeds via Defeconcerted 2-H atom transfers, i.e. the pathway incorporates only intermediates at 0^{th}, 2^{nd}, 4^{th}, 6^{th}, 8^{th} H atom transfer **(blue)** in Fig. 6, without the formation of specific intermediates in between. This alternative pathway is similar to the one supported by another theoretical study[40] but with a lack of experimental support,[8] and it is not clear from Fig. 6 what experiment can be performed to provide evidence. On the basis of literature, a third possibility is the formation of methoxy radical (OCH_3) from H_2CO, where OCH_3 has also been reported in ref [7], and is part of the mechanism of methanation of CO_2 on Cu surface determined from DFT calculations.[57] OCH_3 is not included in Fig.6, but it is expected that this alternative path would also have the difficulty to cleave the C-O bond to generate CH_3, and the OCH_3 may prefer hole scavenging.[60]

A few effects of the reaction environment are not encompassed in our computation but may affect our prediction. The solvent molecules can stabilize strongly some of the species via, for example, H-bonding (the key intermediates are neutral so there are no major differences expected in the polarization energy). However it can be noted that, considering the typical H-bond energy in water (~< 0.4 eV),[67] it is not possible to alter significantly the relative energies of the landscape depicted in Fig. 6. The mechanism may also be interfered by other possible species formed in side reactions, such as carbonates, hydrogen molecules and hydroxyl radicals.[8] Surface defects may also alter the mechanism and/or the energetics of the mechanism prominently. It has been suggested that in the presence of oxygen vacancy CO is more easily formed,[26,68] and the pathway would be more similar to the carbene pathway.[40]

The results presented alongside the tests performed to rule out important computation errors allow the identification of a reaction path among three that is clearly more favourable. As noted above the energy difference between intermediates is sufficiently large and the barriers sufficiently low that the detailed investigation of alternative mechanisms for the elementary reaction steps would not change the conclusion for the given energy landscape. It should be noted that the study of the direct non-adiabatic electron transfer from the defect requires a very different type of study from the one we presented. Possibly the study should focus on a single reduction step and the other mechanisms it could follow, such as electron followed by proton transfer, protonation followed by electron transfer, concerted proton-electron transfer, and multi-electron transfer as proposed in previous theoretical studies [7,39,40] but deemed unlikely [8,39,69]and without strong experimental support. Each elementary step will require adjustment to standard DFT, such as constrained DFT[70,71] for electron localization, and/or a periodic charged slab with background compensating charge that the energy may depend on the width of the vacuum layer in the simulation box.[72] Alternative model for the charged slab can perhaps be the adsorption of H atom on anatase(101),[39] but the treatment of localization of the excess electron would require relatively costly computational method such as DFT+*U*, and the results would be dependent on the *U* value employed.[39,73] Thus, a possible strategy for investigating photocatalytic reaction mechanisms is to consider initially a broad exploration of global reaction mechanisms, as presented in this study, followed by an in-depth study of some elementary step, when necessary.

In conclusion, we have investigated theoretically three proposed reaction mechanisms for the photo-catalytic reduction of CO_2 to gain CH_4 (Eq. 1) on defect-free TiO_2 anatase(101) with first-principles DFT calculations, and we determined that the formaldehyde pathway is the most likely on the basis of a greater thermodynamic stability of the intermediates. Formaldehyde is a thermodynamically preferred intermediate to form in the hydrogenation of CO and the hydrogenation of HCO, over C atom in the carbene pathway and glyoxal in the glyoxal pathway respectively. Our computational approach appears to be useful for both developing sensible mechanistic hypothesis and designing experiments to validate them.

Acknowledgment This research was funded by EPSRC and ERC. We are grateful to Rocco Fornari for comments on this manuscript.

Reference

1 *Int. Energy Agency World Energy Outlook 2015*, 2015, http://www.worldenergyoutlook.org/weo2015/.

2 E. J. Maginn, *J. Phys. Chem. Lett.*, 2010, **1**, 3478.

3 M. Mikkelsen, M. Jørgensen and F. C. Krebs, *Energy Environ. Sci.*, 2010, **3**, 43.

4 M. R. Hoffmann, S. T. Martin, W. Choi and D. W. Bahnemannt, *Chem. Rev.*, 1995, **95**, 69.

5 A. L. Linsebigler, G. Lu and J. T. Yates, *Chem. Rev.*, 1995, **95**, 735.

6 W. Y. Teoh, J. a. Scott and R. Amal, *J. Phys. Chem. Lett.*, 2012, **3**, 629.

7 N. M. Dimitrijevic, B. K. Vijayan, O. G. Poluektov, T. Rajh, K. A. Gray, H. He and P. Zapol, *J. Am. Chem. Soc.*, 2011, **133**, 3964.

8 S. N. Habisreutinger, L. Schmidt-Mende and J. K. Stolarczyk, *Angew. Chem. Int. Ed.*, 2013, **52**, 7372.

9 J. Tang, J. R. Durrant and D. R. Klug, *J. Am. Chem. Soc.*, 2008, **130**, 13885.

10 K. Li, X. An, K. H. Park, M. Khraisheh and J. Tang, *Catal. Today*, 2014, **224**, 3.

11 H. Kato, K. Asakura and A. Kudo, *J. Am. Chem. Soc.*, 2003, **125**, 3082.

12 Z. P. Liu and P. Hu, *J. Chem. Phys.*, 2001, **115**, 4977.

13 Z. P. Liu and P. Hu, *J. Am. Chem. Soc.*, 2003, **125**, 1958.

14 J. K. Nørskov, T. Bligaard, J. Rossmeisl and C. H. Christensen, *Nat. chem.*, 2009, **1**, 37.

15 S. Bai, J. Jiang, Q. Zhang and Y. Xiong, *Chem. Soc. Rev.*, 2015, **44**, 2893.

16 M. Anpo, H. Yamashita, Y. Ichihashi and S. Ehara, *J. Electroanal. chem.*, 1995, **396**, 21.

17 T. Inoue, A. Fujishima, S. Konishi and K. Honda, *Nature*, 1979, **277**, 637.

18 I. A. Shkrob, T. W. Marin, H. He and P. Zapol, *J. Phys. Chem. C*, 2012, **116**, 9450.

19 K. Koci, L. Obalova and O. Solcova, *Chem. Process Eng.*, 2010, **31**, 395.

20 C. C. Yang, Y. H. Yu, B. van der Linden, J. C. S. Wu and G. Mul, *J. Am. Chem. Soc.*, 2010, **132**, 8398.

21 N. M. Dimitrijevic, I. A. Shkrob, D. J. Gosztola and T. Rajh, *J. Phys. Chem. C*, 2012, **116**, 878.

22 G. R. Dey and K. Pushpa, *Res. Chem. Intermed.*, 2007, **33**, 631.

23 I. A. Shkrob, N. M. Dimitrijevic, T. W. Marin, H. He and P. Zapol, *J. Phys. Chem. C*, 2012, **116**, 9461.

24 J. Rasko and F. Solymosi, *J. Phys. Chem.*, 1994, **98**, 7147.

25 V. P. Indrakanti, H. H. Schobert and J. D. Kubicki, *Energy Fuels*, 2009, **23**, 5247.

26 L. Liu, H. Zhao, J. M. Andino and Y. Li, *ACS Catal.*, 2012, **2**, 1817.

27 C. C. Lo, C. H. Hung, C. S. Yuan and J. F. Wu, *Sol. Energ. Mat. Sol.*, 2007, **91**, 1765.

28 A. J. Nozik, *Nature*, 1975, **257**, 383.

29 Á. Valdés, Z. W. Qu, G. J. Kroes, J. Rossmeisl and J. K. Nørskov, *J. Phys. Chem. C*, 2008, **112**, 9872.

30 J. K. Nørskov, J. Rossmeisl, A. Logadottir, L. Lindqvist, J. R. Kitchin, T. Bligaard and H. Jónsson, *J. Phys. Chem. B*, 2004, **108**, 17886.

31 Y. F. Li, Z. P. Liu, L. Liu and W. Gao, *J. Am. Chem. Soc.*, 2010, **132**, 13008.

32 X. Shen, Y. Small, J. Wang, P. Allen, M. Fernandez-Serra, M. Hybertsen and J. Muckerman, *J. Phys. Chem. C*, 2010, **114**, 13695.

33 A. V Akimov, A. J. Neukirch and O. V Prezhdo, *Chem. Rev.*, 2013, **113**, 4496.

34 J. Chen, Y. F. Li, P. Sit and A. Selloni, *J. Am Chem. Soc.*, 2013, **135**, 18774.

35 J. Cheng, X. Liu, J. a Kattirtzi, J. VandeVondele and M. Sprik, *Angew. Chem. Int. Ed.*, 2014, **53**, 12046.

36 S. Hammes-Schiffer and A. A. Stuchebrukhov, *Chem Rev*, 2010, **110**, 6939.

37 C. Venkataraman, A. V. Soudackov and S. Hammes-Schiffer, *J. Phys. Chem. C*, 2008, **112**, 12386.

38 B. H. Solis and S. Hammes-Schiffer, *Inorg. Chem.*, 2014, **53**, 6427.

39 H. He, P. Zapol and L. A. Curtiss, *Energy Environ. Sci.*, 2012, **5**, 6196.

40 Y. Ji and Y. Luo, *ACS Catal.*, 2016, **6**, 2018.

41 P. Giannozzi, S. Baroni, N. Bonini, M. Calandra, R. Car, C. Cavazzoni, D. Ceresoli, G. L. Chiarotti, M. Cococcioni, I. Dabo, A. Dal Corso, S. de Gironcoli, S. Fabris, G. Fratesi, R. Gebauer, U. Gerstmann, C. Gougoussis, A. Kokalj, M. Lazzeri, L. Martin-Samos, N. Marzari, F. Mauri, R. Mazzarello, S. Paolini, A. Pasquarello, L. Paulatto, C. Sbraccia, S. Scandolo, G. Sclauzero, A. P. Seitsonen, A. Smogunov, P. Umari and R. M. Wentzcovitch, *J. Phys. Condens. Matter*, 2009, **21**, 395502.

42 N. Martsinovich, D. R. Jones and A. Troisi, *J. Phys. Chem. C*, 2010, **114**, 22659.

43 G. Henkelman, B. P. Uberuaga and H. Jónsson, *J. Chem. Phys.*, 2000, **113**, 9901.

44 A. Michaelides, Z. P. Liu, C. J. Zhang, A. Alavi, D. A. King and P. Hu, *J. Am. Chem. Soc.*, 2003, **125**, 3704.

45 M. Saeys, M. F. Reyniers, G. B. Marin, V. Van Speybroeck and M. Waroquier, *ChemPhysChem*, 2006, **7**, 188.

46 M. M. Islam, M. Calatayud and G. Pacchioni, *J. Phys. Chem. C*, 2011, **115**, 6809.

47 U. Aschauer and A. Selloni, *Phys. Chem. Chem. Phys.*, 2012, **14**, 16595.

48 E. Maggio, N. Martsinovich and A. Troisi, *J. Phys. Condens. Matter*, 2016, **28**, 074004.

49 C. Di Valentin, G. Pacchioni and A. Selloni, *J. Phys. Chem. C*, 2009, **113**, 20543.

50 D. Cheng, F. R. Negreiros, E. Apra and A. Fortunelli, *ChemSusChem*, 2013, **6**, 944.

51 P. R. Schreiner, H. P. Reisenauer, F. C. Pickard IV, A. C. Simmonett, W. D. Allen, E. Mátyus and A. G. Császár, *Nature*, 2008, **453**, 906.

52 E. C. C. Baly, I. M. Heilbron and W. F. Barker, *J. Chem. Soc. Trans.*, 1921, 1025.

53 Y. Hori, R. Takahashi, Y. Yuzuru and A. Murata, *J. Phys. Chem. B*, 1997, **101**, 7075.

54 T. Bligaard, J. K. Nørskov, S. Dahl, J. Matthiesen, C. H. Christensen and J. Sehested, *J. Catal.*, 2004, **224**, 206.

55 R. P. Bell, *Proc. R. Soc. London, Ser. A*, 1936, **154**, 414.

56 M. G. Evans and M. Polanyi, *Trans. Faraday Soc.*, 1936, **32**, 1936.

57 A. A. Peterson, F. Abild-Pedersen, F. Studt, J. Rossmeisl and J. K. Nørskov, *Energy Environ. Sci.*, 2010, **3**, 1311.

58 A. Vittadini, A. Selloni, F. P. Rotzinger and M. Grätzel, *J. Phys. Chem. B*, 2000, **104**, 1300.

59 H. Liu, M. Zhao, Y. Lei, C. Pan and W. Xiao, *Comp. Mater. Sci.*, 2012, **51**, 389.

60 M. Shen and M. A. Henderson, *J. Phys. Chem. Lett.*, 2011, **2**, 2707.

61 M. A. Henderson, *Surf. Sci. Rep.*, 2011, **66**, 185.

62 Q. Cao, S. Berski, Z. Latajka, M. Räsänen and L. Khriachtchev, *Phys. Chem. Chem. Phys.*, 2014, **16**, 5993.

63 A. J. Foster and R. F. Lobo, *Chem. Soc. Rev*, 2010, **39**, 4783.

64 S. H. Kim, P. C. Stair and E. Weitz, *Langmuir*, 1998, **14**, 4156.

65 J. Cunningham and A. L. Leahy, *J. Phys. Chem.*, 1972, **76**, 2353.

66 M. E. Pronsato, C. Pistonesi, A. Juan, A. P. Farkas, L. Bugyi and F. Solymosi, *J. Phys. Chem. C*, 2011, **115**, 2798.

67 S. J. Suresh and V. M. Naik, *J. Chem. Phys.*, 2000, **113**, 9727.

68 D. C. Sorescu, W. A. Al-Saidi and K. D. Jordan, *J. Chem. Phys.*, 2011, **135**, 124701.

69 P. V. Kamat, *J. Phys. Chem. Lett.*, 2012, **3**, 663.

70 B. Kaduk, T. Kowalczyk and T. Van Voorhis, *Chem. Rev.*, 2012, **112**, 321.

71 E. Poli, J. D. Elliott, L. E. Ratcliff, L. Andrinopoulos, J. Dziedzic, N. D. M. Hine, A. A. Mostofi, C. K. Skylaris, P. D. Haynes and G. Teobaldi, *J. Phys. Condens. Matter*, 2016, **28**, 074003.

72 Y. F. Li, U. Aschauer, J. Chen and A. Selloni, *Acc. Chem. Res.*, 2014, **47**, 3361.

73 E. Finazzi, C. Di Valentin, G. Pacchioni and A. Selloni, *J. Chem. Phys.*, 2008, **129**, 154113.

Toc graphic:

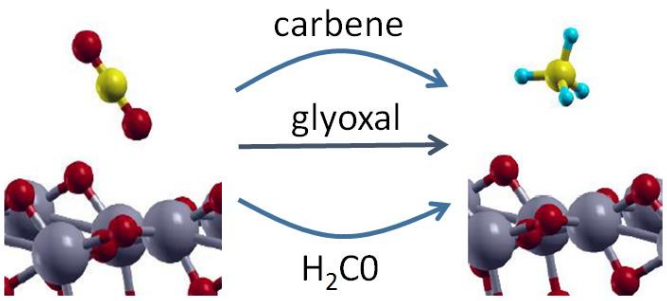

Three reaction pathways for the photocatalytic reduction of carbon dioxide to methane are investigated with density functional theory calculations